Acta Cryst. (1973). A**29**, 632

Direct Observation of Point Defects in $Nb_{12}O_{29}$ by High-Resolution Electron Microscopy

BY S. IIJIMA*

Department of Physics, Arizona State University, Tempe, Arizona 85281, *U.S.A.*

AND S. KIMURA AND M. GOTO

National Institute for Researches in Inorganic Materials, Ibaraki, Japan

(*Received* 7 *May* 1973; *accepted* 26 *May* 1973)

Point defects have been observed directly in non-stoichiometric niobium oxides, $Nb_{12}O_{29}$, by high-resolution electron microscopy at a resolution of 3–4 Å. A proposed model for the point defect is a complex composed of two interstitial metal atoms and two interstitial oxygen atoms. Observations have been made on the annealing out of these defects under electron irradiation. Evidence on the density of these defects offers a semi-quantitative explanation of how the non-stoichiometric oxygen excess in these oxides is accommodated in the matrix structure.

Introduction

During the past few years, electron microscopy has become a useful technique for investigating structural defects in some transition-metal oxides (Allpress, Sanders & Wadsley, 1969). Under highly controlled imaging conditions, structural information has been obtained from Nb, Nb–W, Nb–Zr and Nb–Ti oxides at a resolution of about 3 Å (Iijima, 1971, 1973) and also unknown structures have been derived in some cases from high-resolution microscope images (Iijima & Allpress, 1973*a*; Allpress, Iijima, Roth & Stephenson, 1973). The contrast in these images is directly related to the charge-density distributions within the structures, projected along the incident electron-beam direction (Cowley & Iijima, 1972). It can therefore be expected that in favorable cases point defects within lines of atoms along the incident-beam direction may be imaged at this resolution.

Non-stoichiometry in various compounds derived from Nb_2O_5, based on the ReO_3 structure, has been intensively studied by a German group (Gruehn, 1972). It has been hitherto found (Schäfer, Bergner & Gruehn, 1969) that five compounds, namely $Nb_{12}O_{29}$, $Nb_{22}O_{54}$, $Nb_{47}O_{116}$, $Nb_{25}O_{62}$ and $Nb_{53}O_{132}$, exist in the composition range between NbO_2 and Nb_2O_5. They occur as distinct phases and their structures are closely related. One anomalous feature of these compounds is that the observed oxygen–metal ratios of structurally well defined phases often disagree with the ideal compositions corresponding to a perfect lattice which does not show a measurable lattice expansion.

Since Wadsley defects and coherent intergrowths of neighboring phases were found to be an important source of deviations from stoichiometry in the system WO_3–Nb_2O_5 (Allpress, Sanders & Wadsley, 1969), the classical concept of the solid solution in Nb oxides given by Goldschmidt (1967) has not been given much consideration, probably because of the difficulty of detecting such defects. However, recent work by Allpress & Roth (1971) indicated that Wadsley defects were not the only means of accommodating departures from stoichiometry, and these authors suggested that there could also be some kinds of point defects in these compounds with non-stoichiometric compositions.

During an investigation of phase equilibria in the system NbO_2–Nb_2O_5 by Kimura (1973), it was found that the composition of the $Nb_{12}O_{29}$ phase always deviated slightly toward oxygen excess when it was derived by oxidizing NbO_2. X-ray analyses of this phase showed no trace of neighboring phases, and it has been expected, therefore, that it must either contain Wadsley defects, or some kinds of point defects to accommodate the deviation from the ideal composition.

In this paper, as a part of a series of experiments on the NbO_2–Nb_2O_5 system conducted by high-resolution microscopy, point defects in the $Nb_{12}O_{29}$ phase will be described as one of the possible origins of the existence of such a narrow range of homogeneity observed in the phase diagram.

Experimental

The samples of $Nb_{12}O_{29}$ of black color were part of a series of preparations used by one of the present authors to study the stabilities of phases present in the system NbO_2–Nb_2O_5. The detailed preparation procedures are shown elsewhere (Kimura, 1973). They were obtained by oxidizing NbO_2 at 1400 °C under a controlled atmosphere by using a CO_2/H_2 gas mixture. Their measured compositions were $NbO_{2.418}$ and $NbO_{2.419}$. The oxygen content of the specimens was determined by observing the weight gain when heated to Nb_2O_5 in air at 1000 °C for 3 h.

The samples were ground in an agate mortar and dispersed in acetone. Fragments from the samples were collected on perforated carbon supporting films. Very

* On leave from the Research Institute for Scientific Measurements, Tohoku University, Sendai, Japan.

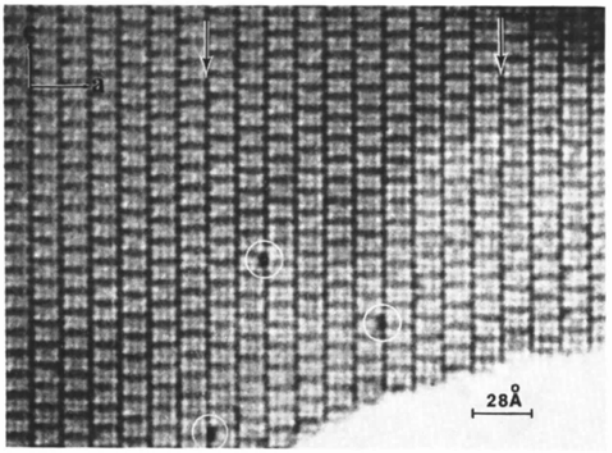

(*a*)

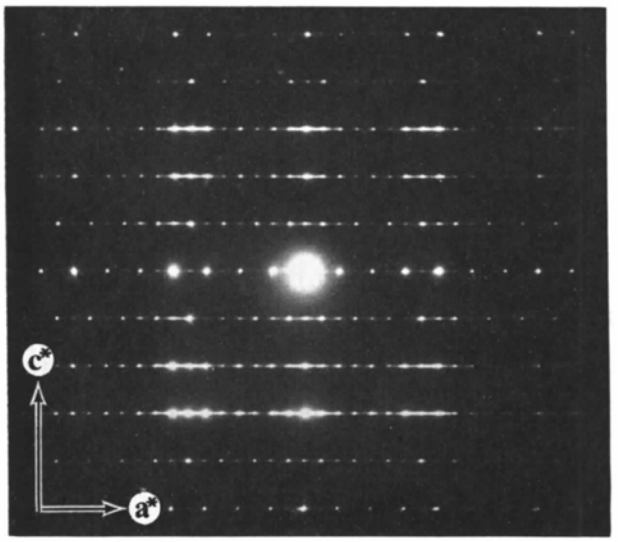

(*b*)

Fig. 2. (*a*) High-resolution two-dimensional lattice image of orthorhombic $Nb_{12}O_{29}$ taken from a fragment of $Nb_{12}O_{29}$ having excess oxygen. Microdomains of monoclinic structure of $Nb_{12}O_{29}$ (arrowed) parallel to the *c* axis are seen. Black spots (encircled) indicate some kinds of point defects. (*b*) Electron-diffraction pattern from the sample as (*a*). Strong spots are those from orthorhombic structure of $Nb_{12}O_{29}$. Streaks result from occurrence of microdomain intergrowths of monoclinic $Nb_{12}O_{29}$ as revealed in (*a*).

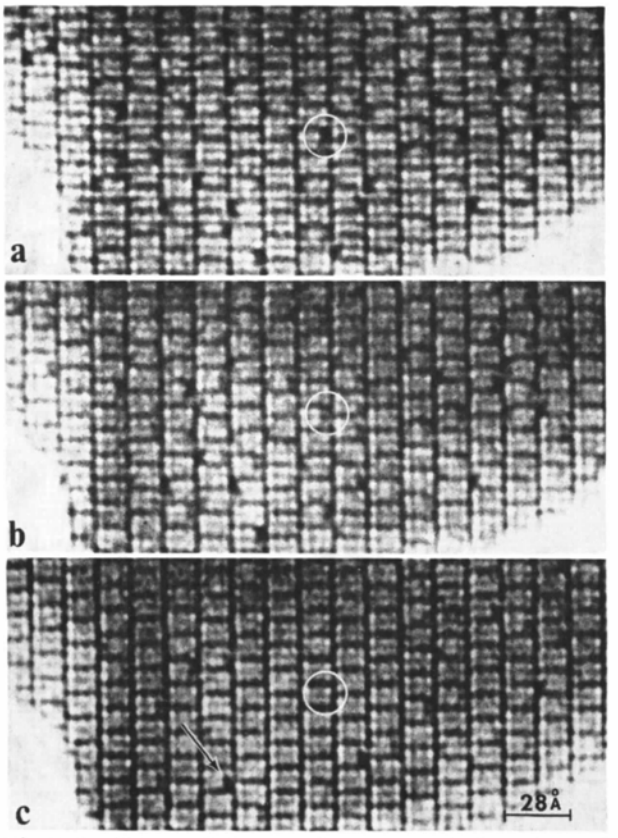

Fig. 3. (*a–c*) Series of pictures taken at several-minute intervals showing the effect of electron irradiation on the black spots.

[*To face p.* 632

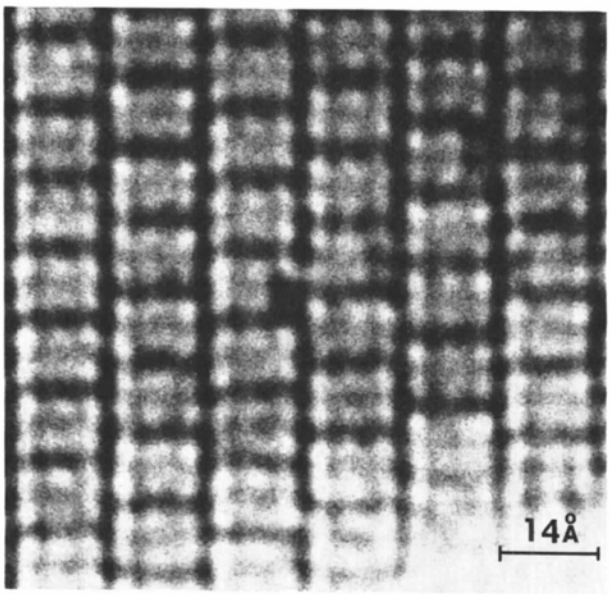

(*a*)

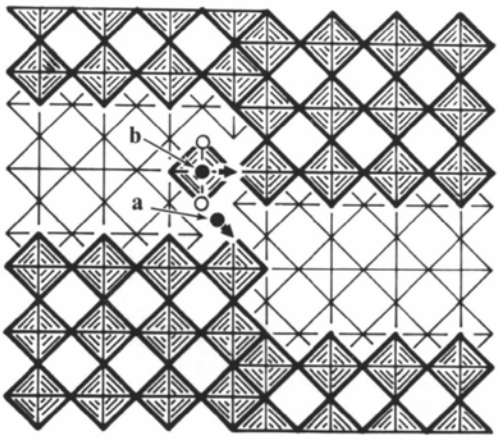

(*b*)

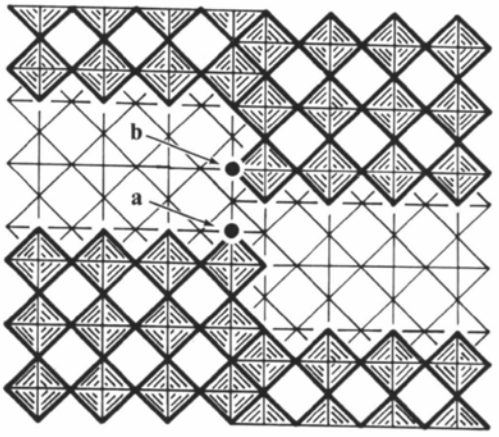

(*c*)

Fig. 4. (*a*) Enlarged image of the black spot appearing in Fig. 3(*c*). The position of the spot corresponds to one of the 2×3 channels in a block. (*b*) A proposed model for the point defect derived from the image shown in Fig. 4(*a*). The point defect is a complex composed of two interstitial metal atoms (indicated by *a* and *b*) and two oxygen atoms (open circles). (*c*) Perfect structure corresponding to the one in (*b*).

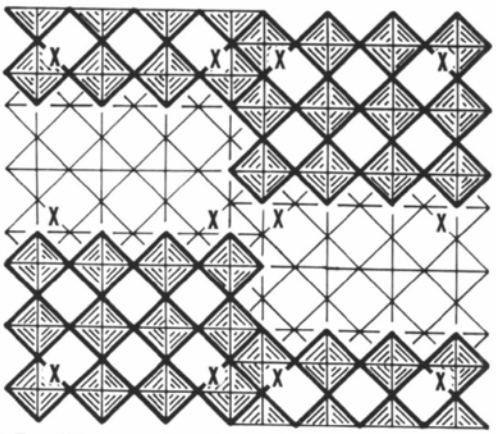

Fig. 5. Possible sites for the point defect in the unit cell (indicated by $\times$).

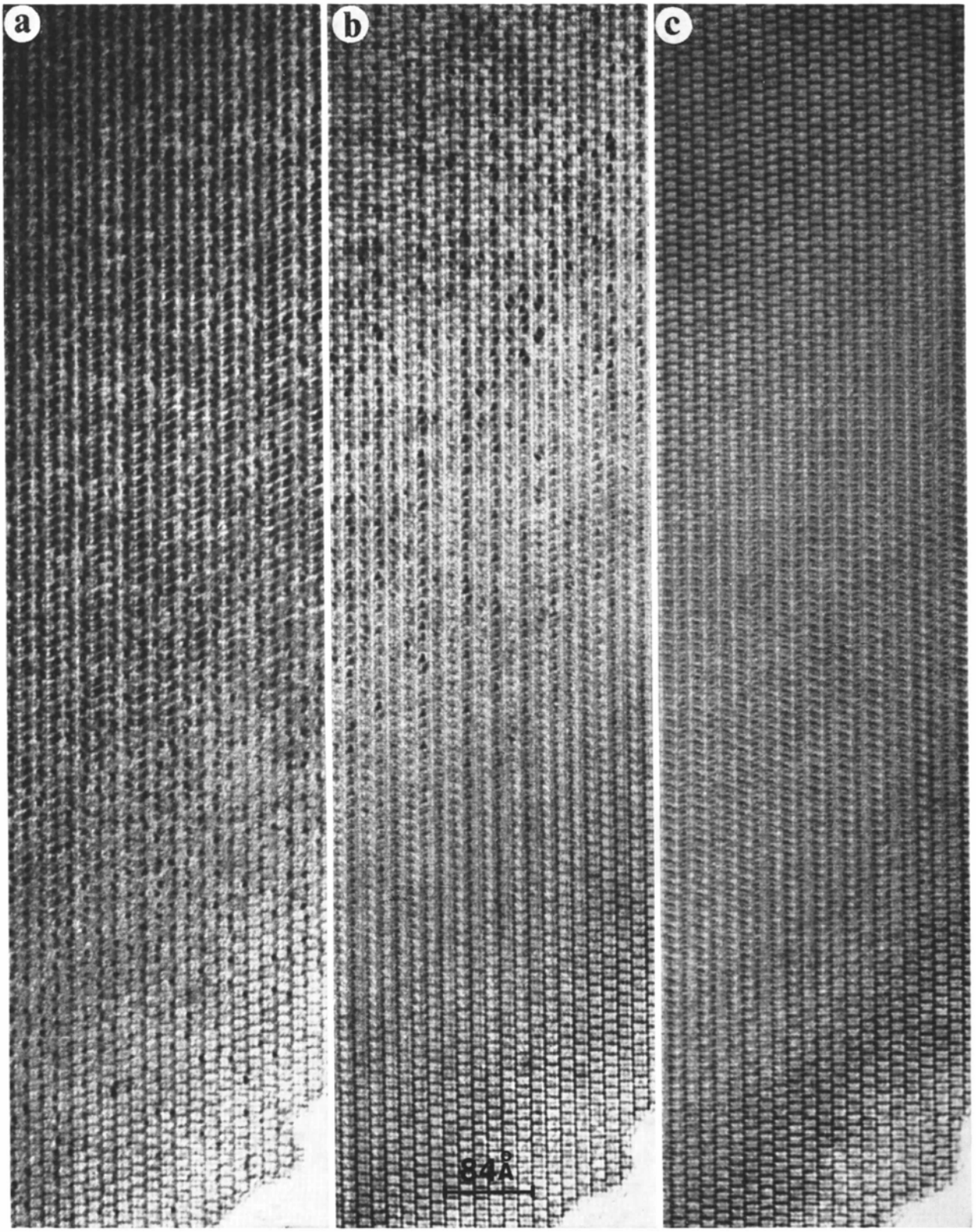

Fig. 6. Series pictures of relatively low-magnification images showing the effects of electron irradiation, from which the density of the point defects could be estimated. (*a*) very early stage of the irradiation. (*b*) after 20 min irradiation (*c*) after intense electron irradiation achieved by taking out the condenser aperture of the microscope.

thin crystal edges projecting over holes were chosen and the specimens were tilted and rotated until the crystals gave exactly symmetrical *h0l* diffraction patterns. Observations were made in a JEM-100B electron microscope, as described previously (Iijima, 1973). Micrographs were recorded by using about 150 contributing diffracted beams and the focusing condition was about 900 Å under focus from the Gaussian image plane. In order to study the effects of electron irradiation on the point defects, an intense electron beam was obtained by taking out the condenser aperture of the electron microscope.

Results and interpretation

We examined three different samples of $Nb_{12}O_{29}$ whose compositions are $NbO_{2.418}$, $NbO_{2.419}$ and $NbO_{2.422}$; the ideal composition is $NbO_{2.417}$. Some fragments from the last sample showed the next-neighboring phase of $Nb_{22}O_{54}$, but none of the fragments from the first two samples showed any intergrowths of the other phases. To clarify the present subject, we will confine ourselves to the observations of only these two samples. However, we could not find any distinguishable structural differences between these two compositions, so that we do not mention which samples were used for the following images.

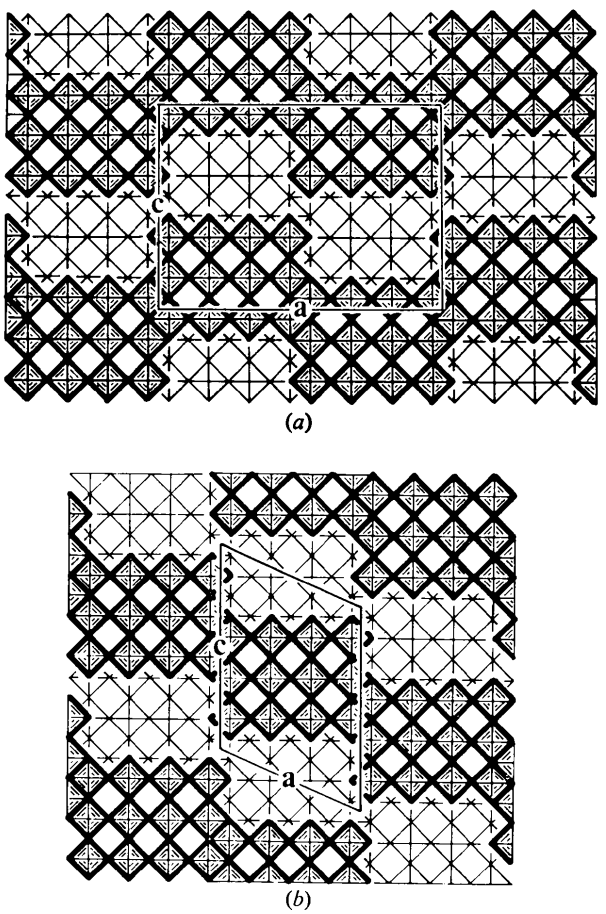

Fig. 1. (*a*) Idealized structure of orthorhombic $Nb_{12}O_{29}$. The darker and lighter squares represent octahedra of NbO_6 which form 3×4 blocks by their corner sharing. They are centered about the two levels perpendicular to the *b* axis and are 1·9 Å apart. The unit cell in projection is outlined ($a=28{\cdot}90$, $b=3{\cdot}835$, $c=20{\cdot}72$ Å). (*b*) Structure of monoclinic $Nb_{12}O_{29}$. The unit cell is outlined ($a=15{\cdot}66$, $b=3{\cdot}832$, $c=20{\cdot}72$ Å and $\beta=112{\cdot}93°$).

It has been shown by X-ray analysis that there are orthorhombic and monoclinic polymorphs of $Nb_{12}O_{29}$, (Norin, 1963, 1966), isostructural with $Ti_2Nb_{10}O_{29}$ (Wadsley, 1961). Fig. 1(*a*) represents a *b*-axis projection of the idealized model of the orthorhombic structure, showing the structure as composed of 3×4 blocks of corner-shared metal–oxygen octahedra, based on the rhenium trioxide structure. The blocks drawn dark and light alternate along the *b*-axis direction giving an axial length $b=3{\cdot}835$ Å. The projection of the unit cell indicated by lines has dimensions $a=28{\cdot}90$ and $c=20{\cdot}72$ Å. Fig. 1(*b*) represents the structure of monoclinic $Nb_{12}O_{29}$ in a similar way. The unit cell has the dimensions $a=15{\cdot}66$,* $b=3{\cdot}832$, $c=20{\cdot}72$ Å and $\beta=112{\cdot}93°$.

A two-dimensional lattice image of orthorhombic $Nb_{12}O_{29}$ taken by a high-resolution microscope is reproduced in Fig. 2(*a*). The similarity of the projection with the image is apparent. The appearance of the image is almost the same as the one taken from orthorhombic $Ti_2Nb_{10}O_{29}$ which was previously reported by one of the present authors (Iijima, 1971). Fig. 2(*b*) shows a typical electron-diffraction pattern taken from the fragment of the $Nb_{12}O_{29}$, where the strong spots are those from the orthorhombic structure. Appreciable streaks are seen along the a^* axis. One can immediately expect the existence of a number of fault planes parallel to the *c* axis. These can be recognized in Fig. 2(*a*), where they are seen to be microdomains (arrowed) composed of one unit-cell width of the monoclinic phase.† Most fault bands are composed of one or more unit cells in width and distributed randomly. These defects do not alter the composition of the crystal. When the fault band is one block wide it can be regarded as a stacking fault on (100) planes. This confirms Norin's results that all the $Nb_{12}O_{29}$ samples he prepared were mixtures of the monoclinic and orthorhombic modifications (Norin, 1963). Similar frequent occurrences of these intergrowths have also been found in fragments of orthorhombic and monoclinic $Ti_2Nb_{10}O_{29}$ (Allpress, 1969).

A particularly interesting finding in this study is that black spots [encircled in Fig. 2(*a*)] are frequently observed within a block. Their shapes and contrast are extremely sensitive to crystal orientation, focusing and total exposure time. Fig. 3(*a*), (*b*) and (*c*) shows a series of pictures of the same area containing the black spots,

* In Norin's original paper (1966), *a* is 31·31 Å, *i.e.* twice as large.

† The reader should look along the *a* axis with the Figure inclined to the line of sight.

in which corresponding positions are encircled. They were taken successively at several-minute intervals under carefully controlled imaging conditions. Most of these black spots disappear with exposure time. However the black spot which is marked by an arrow in Fig. 3(*c*) appears to be present in (*a*) and (*c*), but absent in (*b*). An enlarged image of one of black spots in Fig. 3(*c*) is reproduced in Fig. 4(*a*). The shape of the black spot is a quite distinctive square of about 6×6 Å, which is located at the position corresponding to one of the tunnels in a 3×4 block (see Fig. 1). From our previous experience, we know that when we look at the very thin edges of the crystals (less than 150 Å), the black-contrast regions correspond to the higher-charge-density regions of the structure projected along the incident electron-beam direction. Therefore we can say immediately that this black contrast might be caused by the presence of additional atoms. Thus it may be supposed intuitively that interstitial metal atoms exist at the positions correponding to tunnels of the ReO_3-type lattice. This simple model, however, does not explain the fact that our samples must have an oxygen excess. A reasonable model for this defect should include incorporation of extra oxygen atoms into the matrix, because the present samples did not show any structural defects or microdomain intergrowths which contribute to the deviation of the composition. Furthermore the appearance of the black spots seems to be similar to that of the tetrahedral sites previously observed in *H*-Nb_2O_5 and $TiNb_{24}O_{62}$ (Iijima, 1973; Iijima & Allpress, 1973*b*) and the defects disappear easily with electron irradiation.

We arrived at a model for this defect which satisfies the several requirements mentioned above. A proposed model is represented in Fig. 4(*b*). It is a complex of two interstitial niobium atoms and two interstitial oxygen atoms. One metal atom (indicated by *a*) has exactly the same tetrahedral coordination as is found in higher oxides of niobium. Another metal atom (indicated by *b*) having octahedral coordination can be regarded as a part of the 3×4 block but it has two oxygen atoms unshared with other octahedra (indicated by open circles). If these two oxygen atoms are released and the two metal atoms are displaced by $\mathbf{b}/\sqrt{2}$ along $[\frac{1}{7}\bar{1}0]$ and $\sqrt{3}b/4$ along $[\frac{1}{7}\bar{1}\frac{1}{5}]$ respectively, as indicated by arrows in the Figure, one can have a perfect structure of $Nb_{12}O_{29}$ [Fig. 4(*c*)]. Therefore the metal atoms in the defect are in fact part of the ordered structure, and have moved into interstitial positions in order to stabilize the presence of additional oxygen atoms. A similar displacement of the metal atoms has been suggested by Andersson & Wadsley (1966). They proposed a number of these types of displacements of atoms in their model for 'cooperative diffusion' in the crystallographic shear structures in the block structure, based on the ReO_3 structure. The disappearance of the black spots during the observation indicates that this displacement has occurred easily in the electron microscope. By examining numerous photographs, it was found that these black spots can occur only at the crystallographically equivalent positions in the unit cell which are indicated by $\times$ in Fig. 5.

So far we have interpreted the observations from a two-dimensional point of view. Now it will be necessary to make clear whether black spots are caused by the existence of isolated point defects or by chains of point defects parallel to the *b* axis. In high-resolution microscopy, it is inevitable that the specimens suffer radiation damage or heating effects from the extremely intense electron-beam irradiation during the observation. Therefore, in order to get some quantitative information on the defect density, it is necessary to observe the fragments at a very early stage of irradiation. This experiment is extremely difficult because it takes at least several minutes to set the crystal at the *b*-axis orientation in a goniometer stage of the microscope. By keeping this in mind, a series of pictures showing the effects of radiation on the point defects was recorded with minimum-intensity beam, where it was confirmed that no measurable decrease in the number of black spots was observed. One of these images is shown in Fig. 6(*a*). The density of the black spots increases towards the thicker part of the crystal (top of the image). This suggests that the black spots should not be due to continuous chains of point defects through the crystal but rather are due to isolated defects or chains of defects of limited length. Fig. 6(*b*) shows the image taken from the same area after 20 min irradiation. The black spots can hardly be seen except in the thicker region of the crystal. Fig. 6(*c*) shows the image taken after intense electron-beam irradiation achieved by removing the condenser aperture of the microscope. All black spots have completely disappeared.

It may be noted here that Fig. 6(*c*) shows the repetition of the clear image of the block structure in the thicker region of the crystal. This phenomenon has been found previously as a characteristic of high-resolution two-dimensional lattice images of particular block structures (Cowley, Iijima & Fejes, 1973). The contrast in the thin region (up to 150 Å thickness) reappears in the thicker region whose thickness is estimated to be about 700–1000 Å.* Therefore, this series of pictures makes it possible to estimate roughly the density of the defects. The thickness, at which black spots are seen in every 3×4 block image in Fig. 6(*a*), was estimated to be about 500 Å from Fig. 6(*c*) by postulating that the crystal has wedge shape. Thus there are 130 unit cells in a column parallel to the *b* axis. If one black spot is caused by the presence of one point defect in one column of the 3×4 block through the crystal, at least four point defects for 130 unit cells should be present. These pictures were taken from the fragment with composition $NbO_{2.419}$. Supposing that the

* Thickness determinations of the crystal were made by the observation of the images of planar defects for various tilts of the crystal.

deviation of the composition of the $NbO_{2.419}$ from the ideal $NbO_{2.417}$ can be accommodated by only including the presently proposed point defects, a simple calculation indicates that the specimen should contain one point defect for 20 unit cells. This is in agreement with the observed value within experimental error. Consequently it can be concluded that one black spot is associated with one or two point defects. We did not observe the fragments with composition $NbO_{2.418}$ to compare with the above results but we are confident that more time and patience will give us more quantitative data on this problem.

Discussion

The two-dimensional lattice imaging technique has been recognized for the past few years as a useful means for obtaining structural information on both one- and two-dimensional defects in some transition-metal oxides. The present study verified further that this technique could be extended to detect point defects in those oxides. Traditionally, point defects in solids have been studied indirectly by measuring electrical conductivities, lattice expansions and some other physical quantities, and then analyzing the data in terms of an assumed point-defect structure. We believe that high-resolution microscope observations could be a promising method for investigating this problem directly.

Image contrast

Since our images are recorded from very thin crystals (less than 150 Å) by using many diffracted beams (150 beams), the image contrast should be dealt with as for a phase object. This is essentially different from the usual 'diffraction contrast'. It has been known that faulted regions in a crystal can be imaged as well as ordered regions. This fact suggests that the dynamical scattering of the electrons can be treated by a column approximation, where effects of all diffracted beams are confined within a column of about 3–5 Å diameter through the crystal (Fejes, Iijima & Cowley, 1973). Observation of the black spot [Fig. 3(*c*)] gives a further confirmation of this basis for treatment of the image contrast. Theoretical interpretation of perfect two-dimensional lattice images of some block structures has been quantitatively studied by O'Keefe (1973) and Fejes (1973) and a fairly good agreement with experiments has been obtained for dependence of the image contrast on crystal thickness, focusing and other electron-optical parameters. It was found from this experiment that the contrast of the black spot is associated with only one or two point defects. It is conceivable that the main contribution to the contrast of the point defect is due to slightly displaced metal atoms and their surrounding metal atoms. For further discussion, we should wait until a theoretical calculation shows how many point defects are required to give distinguishable contrast in a matrix lattice.

Defect formation

We are confident that Fig. 6(*c*) which was taken after intense electron irradiation shows the image of an almost perfect lattice of $Nb_{12}O_{29}$ except for some microdomains of the monoclinic phase. According to the presently proposed model for the point defect, when the point defect disappears during the electron irradiation, liberation of two oxygen atoms for one defect should occur in the crystal. $Nb_{12}O_{29}$ is known to be very easily oxidized and its equilibrium oxygen pressure for reduction is known to be very low (Kimura, 1973; Schäfer, Bergner & Gruehn, 1969). This fact, however, would not be in contradiction to the present model because a carbon-deposition reaction with oxygen on the surface of specimens in the microscope is inevitable during observation. The excess oxygen atoms are located at a 'quasi-tetrahedral site' in the point defect which might be unstable. It is acceptable that these oxygen atoms are readily released from the site and migrate to the crystal surface to escape into the vacuum, in the form of gas species which are byproducts of the carbon-deposition reaction, when the specimen is heated or has enhanced diffusion rates owing to electron irradiation [Fig. 6(*c*)]. This procedure should be accompanied simultaneously by a slight rearrangement of the metal atoms. Such a small displacement of metal atoms is also probable at high temperature. These changes could possibly occur in the opposite way with a small probability during diffusion of released oxygen atoms so that a 'quasi-tetrahedral site' would be formed. This is supported by observation of the appearance of a black spot during electron irradiation [Fig. 3(*c*)].

It may be possible to regard our oxygen-excess samples as a transition state from $Nb_{12}O_{29}$ to $Nb_{22}O_{54}$ which is the next higher oxide in the phase diagram. Furthermore it may be speculated that if we introduce many more oxygen atoms into the present system, the 'quasi-tetrahedral sites' could be stabilized by structural rearrangement of the block structure, that is, 'crystallographic shear'. We could not detect short-range ordering of the point defects but its possibility seems to be expected as an initial state of long-range ordering of the next-higher oxides of $Nb_{22}O_{54}$.

Non-stoichiometry

It has been made clear that the point defects play a major role in non-stoichiometry of $Nb_{12}O_{29}$. The proposed model for the point defects could explain somewhat quantitatively the deviation of the oxygen-excess sample of $Nb_{12}O_{29}$ from the ideal composition. We believe that this could be a clue to the explanation of the existence of a narrow range of the other higher oxide phases observed in the NbO_2–Nb_2O_5 system which cannot so far be explained by introducing Wadsley defects. This observation will be reported soon.

One of us (S.I.) wishes to thank Professor J. M. Cowley for his continuous encouragement, and to

acknowledge the support of a N.S.F. Area Development Grant in Solid State Science (No. GU 3169). The other two authors are grateful to the remaining members of the Nb–O research group in the NIRIM for their continued interest in and suggestions for this work.

References

ALLPRESS, J. G. (1969). *J. Solid. State Chem.* **1**, 66–81.
ALLPRESS, J. G., IIJIMA, S., ROTH, R. S. & STEPHENSON, N. C. (1973). *J. Solid State Chem.* **7**, 89–94.
ALLPRESS, J. G. & ROTH, R. S. (1971). *J. Solid State Chem.* **3**, 209–216.
ALLPRESS, J. G., SANDERS, J. V. & WADSLEY, A. D. (1969). *Acta Cryst.* B**25**, 1156–1164.
ANDERSSON, S. & WADSLEY, A. D. (1966). *Nature, Lond.* **211**, 581–583.
COWLEY, J. M. & IIJIMA, S. (1972). *Z. Naturforsch.* **27**a, 445–451.
FEJES, P. L. (1973). Ph.D. Thesis of Arizona State Univ.
FEJES, P. L., IIJIMA, S. & COWLEY, J. M. (1973). *Acta Cryst.* A**29**, 710–714.
GOLDSCHMIDT, H. J. (1967). *Interstitial Alloys*, pp. 419–421. London: Butterworths.
GRUEHN, R. (1972). In *Natl. Bur. Stand. Spec. Publ.* 364, *Solid State Chem., Proceeding of the 5th Materials Research Symposium*, pp. 63–86. Edited by R. S. ROTH and S. J. SCHNEIDER.
IIJIMA, S. (1971). *J. Appl. Phys.* **42**, 5891–5893.
IIJIMA, S. (1973). *Acta Cryst.* A**29**, 18–24.
IIJIMA, S. & ALLPRESS, J. G. (1973*a*). *Acta Cryst.* In the press.
IIJIMA, S. & ALLPRESS, J. G. (1973*b*). *J. Solid State Chem.* **7**, 94–105.
KIMURA, S. (1973). *J. Solid State Chem.* **6**, 438–449.
NORIN, R. (1963). *Acta Chem. Scand.* **17**, 1391–1404.
NORIN, R. (1966). *Acta Chem. Scand.* **20**, 871–880.
O'KEEFE, M. (1973). *Acta Cryst.* A**29**, 389–401.
SCHÄFER, H., BERGNER, O. & GRUEHN, R. (1969). *Z. anorg. allgem. Chem.* **365**, 31–50.
WADSLEY, A. D. (1961). *Acta Cryst.* **14**, 664–670.

Acta Cryst. (1973). A**29**, 636

Piezo-Optic Birefringence in CsCl-Structure Crystals

BY RAVINDHARAN ETHIRAJ AND V. G. KRISHNAMURTY
Department of Physics, Osmania University, Hyderabad-500007, *India*

AND K. G. BANSIGIR
Department of Physics, Jiwaji University, Gwalior-470001, *India*

(*Received* 2 *April* 1973; *accepted* 10 *May* 1973)

Following the theoretical approach of Bansigir and Iyengar, expressions for $p_{11}-p_{12}$ and p_{12}/p_{11} are developed for crystals of the CsCl type. Using experimental values of $p_{11}-p_{12}$, the polarizabilities of some of the ions are evaluated. From the calculated values of the polarizabilities, the ratios of the strain-optical constants are evaluated.

Introduction

Expressions for the change in the refractive index due to strain in NaCl-type crystals, were developed by Bansigir & Iyengar (1961). However no such study was made on crystals belonging to the CsCl type. In this paper an attempt has been made to develop the theory for CsCl-type crystals on the lines suggested by Bansigir & Iyengar. Using experimental values of $p_{11}-p_{12}$, (Laiho & Korpela, 1968) the polarizabilities of various ions are calculated and compared with observed values. From the calculated values of α's the ratios of strain-optical constants of a few crystals are evaluated.

Theory

It is well known that when a cubic crystal is stressed, its refractive index changes and varies with direction. This change can be expressed in the following manner.

Let a rectangular bar of the crystal with edges parallel to [100], [010], [001] (to be called X, Y and Z respectively) be stressed along the **Z** direction. The changes dn_x and dn_z in the refractive index n are related to strain ε (along **Z**) through the following expressions based on the phenomenological theory of Pockels (1906), the observation being made along the **Y** direction

$$dn_x = n_x - n = -p_{12}(n^3/2)\varepsilon$$
$$dn_z = n_z - n = -p_{11}(n^3/2)\varepsilon \qquad (1)$$

where n_x and n_z are the refractive indices of the stressed crystal for light vibrating in the **X** and **Z** directions respectively; n is the refractive index of the crystal in its unstrained condition and p_{12} & p_{11} are the respective strain-optical coefficients.